

Articles

Contribution from the Department of Chemistry,
Texas A&M University, College Station, Texas 77843

Carbon Monoxide Ligand Substitutional Processes Involving Anionic Group 6 Metal Carboxylates and Their Relevance to Decarboxylation Mechanisms

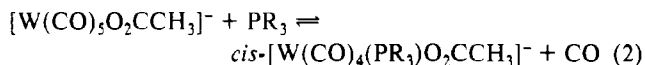
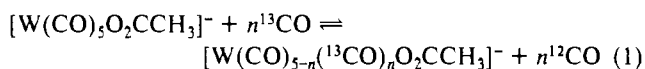
Donald J. Darensbourg* and Holly Pickner Wiegreffe

Received January 12, 1989

Mechanistic aspects of ligand substitution reactions of $[\text{W}(\text{CO})_5\text{O}_2\text{CCH}_3]^-$ complexes with phosphorus donor ligands have been investigated. Kinetic measurements show the process to be first order in metal substrate and nearly zero order in incoming ligand concentration. The activation parameters, determined for the reaction of $[\text{W}(\text{CO})_5\text{O}_2\text{CCH}_3]^-$ with $\text{P}(\text{OCH}_3)_3$ as entering ligand to afford $\text{cis-}[\text{W}(\text{CO})_4(\text{P}(\text{OCH}_3)_3)\text{O}_2\text{CCH}_3]^- + \text{CO}$, are $\Delta H^\ddagger = 23.3 \pm 0.8 \text{ kcal mol}^{-1}$ and $\Delta S^\ddagger = 5.4 \pm 2.6 \text{ eu}$. This facile carbonyl displacement reaction is ascribed, in part, to an intramolecular ligand-assisted dissociation of CO, where the distal oxygen atom of the acetate moiety interacts with the cis CO ligands to effect their selective loss. Consistent with this description, the $[\text{W}(\text{CO})_4(\eta^2\text{-O}_2\text{CCH}_3)]^-$ complex has been synthesized and characterized by infrared and ^{13}C NMR spectroscopies and shown to undergo rapid reactions with incoming ligands (PR_3 and CO) to yield $\text{cis-}[\text{W}(\text{CO})_4(\text{L})\text{O}_2\text{CCH}_3]^-$ compounds. The relevance of CO dissociation and the resultant formation of a chelated acetate ligand to the decarboxylation reactions of the closely related formate derivatives is discussed.

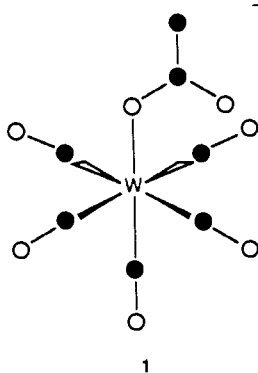
Introduction

We have reported on the solution reactivity of anionic group 6 metal pentacarbonyl acetate complexes toward carbon monoxide displacement with either isotopically labeled CO or phosphorus donor ligands (eq 1 and 2).^{1,2} Both processes occur quite readily

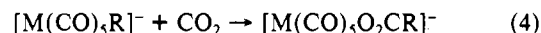
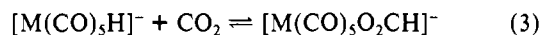


at ambient temperature in tetrahydrofuran solution. Furthermore, it was possible via ^{13}C -NMR spectroscopy to establish that there was stereoselective cis carbonyl loss during the ligand substitution reactions.

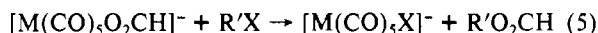
Therefore, the acetate ligand is a cis-labilizing ligand.³ This process might be further facilitated by the distal oxygen atom of the acetate ligand serving as an internal nucleophile and displacing a cis CO ligand with subsequent chelate formation. Indeed, the solid-state structure of $[\text{W}(\text{CO})_5\text{O}_2\text{CCH}_3]^-$ clearly illustrates that the oxygen atom of the acetate moiety is predisposed to interacting with the cis CO ligands (1).



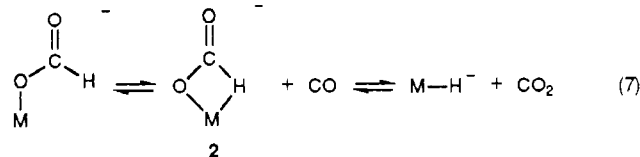
Concomitantly, we have a great deal of interest in group 6 metal carboxylates due to their importance in carbon dioxide chemistry. That is, reactions 3 and 4 are pivotal steps in reduction of carbon



dioxide by way of transition-metal complexes.⁴⁻⁶ Of particular relevance to the above study is the importance of CO dissociation in $[\text{M}(\text{CO})_5\text{O}_2\text{CH}]^-$ and $[\text{M}(\text{CO})_5\text{O}_2\text{CR}]^-$ derivatives in subsequent reactions with dihydrogen⁷ or alkyl halides⁸ to afford the corresponding ester or carboxylic acid (eq 5 and 6).



Of additional consequence is the role of metal unsaturation in decarboxylation reactions (the reverse of reaction 3) of the $[\text{M}(\text{CO})_5\text{O}_2\text{CH}]^-$ derivatives. A $\text{M}(\text{CO})_4[\text{formate}]^-$ intermediate (2) has been proposed in the decarboxylation reaction, where the formate ligand is chelated through an oxygen and a hydrogen atom as is skeletally depicted in eq 7.^{9,10} Hence, a knowledge of the



- (1) Cotton, F. A.; Darensbourg, D. J.; Kolthammer, B. W. S. *J. Am. Chem. Soc.* **1981**, *103*, 398.
 (2) Cotton, F. A.; Darensbourg, D. J.; Kolthammer, B. W. S.; Kudarski, R. *Inorg. Chem.* **1982**, *21*, 1656.
 (3) For a detailed discussion of cis labilization, see: (a) Brown, T. L.; Atwood, J. D. *J. Am. Chem. Soc.* **1976**, *98*, 3160. (b) Lichtenberger, D. L.; Brown, T. L. *J. Am. Chem. Soc.* **1978**, *100*, 366.

- (4) (a) Walther, D. *Coord. Chem. Rev.* **1987**, *79*, 135. (b) Behr, A. In *Catalysis in C₁ Chemistry*; Keim, W., Ed.; Reidel: Dordrecht, The Netherlands, 1983; p 169. (c) Eisenberg, R.; Hendriksen, D. E. *Adv. Catal.* **1979**, *28*, 79. (d) Darensbourg, D. J.; Kudarski, R. *Adv. Organomet. Chem.* **1983**, *22*, 129. (e) Ito, T.; Yamamoto, A. *Organic and Bio-organic Chemistry of Carbon Dioxide*; Inoue, S., Yamazaki, N., Eds.; Kodansha, Ltd.: Tokyo, 1982; p 79. (f) Palmer, D. A.; van Eldik, R. *Chem. Rev.* **1983**, *83*, 651. (g) Sneed, R. P. A. In *Comprehensive Organometallic Chemistry*; Wilkinson, G., Stone, F. G. A., Abel, E. W., Eds.; Pergamon Press: Oxford, England, 1982; Vol. 8, p 225. (h) Kolomnikov, I. S.; Grigoryan, M. Kh. *Russ. Chem. Rev. (Engl. Transl.)* **1978**, *47*, 334. (i) Braunstein, P.; Matt, D.; Nobel, D. *Chem. Rev.* **1988**, *88*, 747.
 (5) Darensbourg, D. J.; Rokicki, A. *Organometallics* **1982**, *1*, 1685.
 (6) Darensbourg, D. J.; Hanckel, R. K.; Bauch, C. G.; Pala, M.; Simmons, D.; White, J. N. *J. Am. Chem. Soc.* **1985**, *107*, 7463.
 (7) Darensbourg, D. J.; Ovalles, C. *J. Am. Chem. Soc.* **1984**, *106*, 3750.
 (8) Darensbourg, D. J.; Ovalles, C. *J. Am. Chem. Soc.* **1987**, *109*, 3330.

kinetic parameters for CO dissociation in $[M(CO)_5O_2CR]^-$ derivatives, coupled with kinetic data for the decarboxylation reaction, should be extremely informative in defining the transition state for C-H bond-forming reactions involving metal hydrides and carbon dioxide.

Our present communication provides kinetic details for the reaction described in eq 2. In addition, spectroscopic identification of the proposed intermediate, $[W(CO)_4(\eta^2-O_2CCH_3)]^-$, has been obtained, as well as its reactivity with incoming ligands.

Experimental Section

Materials. All manipulations were carried out either in an argon drybox or on a double-manifold Schlenk vacuum line. Solvents were dried and degassed prior to use by distillation from sodium benzophenone ketyl under nitrogen. Tetrahydrofuran (THF) and $AgNO_3$ were purchased from J. T. Baker Chemical Co., whereas 2,5-dimethyltetrahydrofuran (2,5-Me₂THF), $Ag_2O_2CCH_3$, PPh_3 , and $P(OCH_3)_3$ were purchased from Aldrich Chemical Co. The phosphine was purified by recrystallization from hot hexane and the phosphite was doubly distilled from sodium benzophenone ketyl under nitrogen, before use. $W(CO)_6$ was purchased from Strem Chemicals, Inc. $NaO_2^{13}CCH_3$ was purchased from B.O.C. Limited. Carbon monoxide was purchased from Matheson Gas Products, Inc., and ^{13}CO (99% enriched) was purchased from Isotec, Inc. The photolysis experiments were performed with a mercury arc 400-W UV immersion lamp, which was purchased from Ace Glass, Inc. IR spectra were recorded on an IBM FTIR/32 spectrometer using 0.1 mm NaCl solution cells. ^{13}C NMR spectra were taken on a Varian XL-200 superconducting high-resolution spectrometer with an internal deuterium lock in 5-mm tubes with THF/acetone-*d*₆ as the solvent mixture. $[PPN][W(CO)_5O_2CCH_3]$ (PPN^+ = bis(triphenylphosphine)-nitrogen(1+) cation) was prepared from $[PPN][O_2CCH_3]$ and $W(CO)_6$ by the reported procedure.^{7,11} $[PPN][W(CO)_5O_2^{13}CCH_3]$ was synthesized from the reaction of $[PPN][W(CO)_5Cl]$ and $AgO_2^{13}CCH_3$, analogous to the literature preparation.² $[PPN][W(^{13}CO)_5O_2CCH_3]$ and $[PPN][W(^{13}CO)_4O_2^{13}CCH_3]$ were prepared by stirring solutions of $[PPN][W(CO)_5O_2CCH_3]$ and $[PPN][W(CO)_5O_2^{13}CCH_3]$, respectively, with ^{13}CO , according to the literature procedure.² $[Et_4N][W(CO)_5O_2CCH_3]$ (Et_4N^+ = tetraethylammonium cation) was prepared from $[Et_4N][W(CO)_5Cl]$ and AgO_2CCH_3 according to the published procedure.¹ $[PPN][Cr(CO)_5O_2CH]$ was prepared from a reaction of CO_2 and $[PPN][Cr(CO)_5H]$.⁹

Kinetic Measurements. The kinetics of carbonyl ligand substitution in $[PPN][W(CO)_5O_2CCH_3]$ by $P(OCH_3)_3$ were monitored by IR spectroscopy. Solution temperatures were controlled by a thermostated water bath, with a precision of ± 0.1 °C. In a typical experiment, to a solution of $[PPN][W(CO)_5O_2CCH_3]$ (0.080 g, 9.0×10^{-5} mol) in THF (6.0 mL) was added $P(OCH_3)_3$ via syringe. Pseudo-first-order conditions were employed with the concentration of phosphite in large (>20-fold) excess over that of the metal complex. Small (~ 0.2 mL) aliquots of the solution were withdrawn periodically and examined by IR spectroscopy. The formation of $[PPN][W(CO)_4(P(OCH_3)_3)O_2CCH_3]$ was followed by measuring the absorbance of the $\nu(CO)$ IR band at 2066 cm^{-1} as a function of time. A base-line correction was made on each spectrum by subtracting the absorbance in a region free from reactant, product, or phosphite peaks. Arbitrarily chosen was the value at 2030 cm^{-1} . Pseudo-first-order rate constants and activation parameters were calculated by using least-squares fitting programs at a 90% confidence limit. The rate constants were determined by plotting $\ln(A_i - A_t)$ versus time, where A_i is the absorbance at infinite time and A_t is the absorbance at time t . Figures 1 and 2 show a plot of $\ln(A_i - A_t)$ vs time t and an Arrhenius plot,¹² respectively. The rate constant for the carbonyl substitution reaction of $[PPN][W(CO)_5Cl]$ with $P(OCH_3)_3$ in THF was measured in a similar manner.

Also examined were the kinetics of carbonyl substitution of $[Et_4N][W(CO)_5O_2CCH_3]$ with $P(OCH_3)_3$ to yield $[Et_4N][W(CO)_4(P(OCH_3)_3)O_2CCH_3]$ in 2,5-Me₂THF. The kinetic technique was modified slightly for these determinations.¹³ The investigations using 2,5-

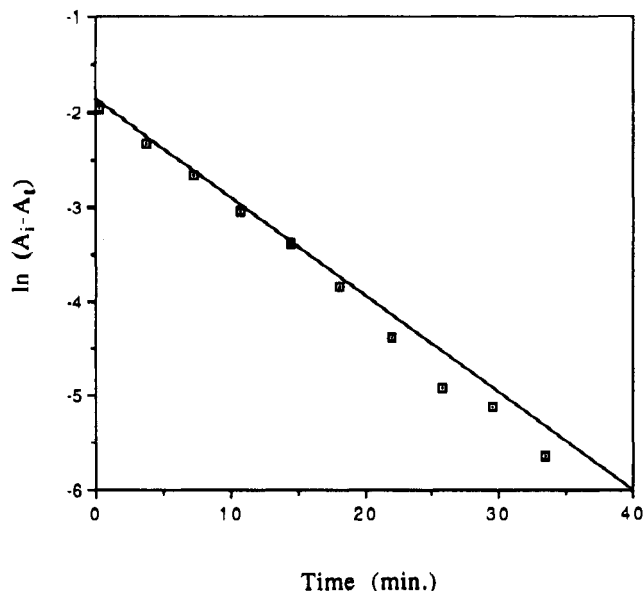


Figure 1. Typical data plot for the ligand substitution reaction of $[PPN][W(CO)_5O_2CCH_3]$ with $P(OCH_3)_3$ at 31.9 °C, under pseudo-first-order conditions.

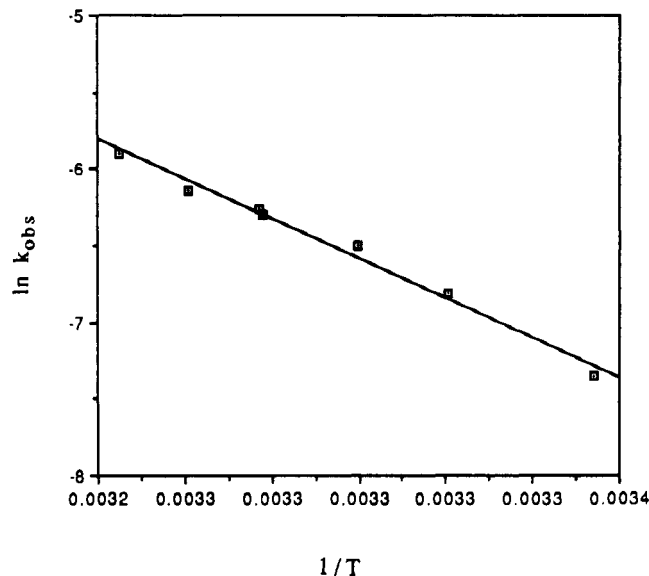


Figure 2. Arrhenius plot for the ligand substitution reaction of $[PPN][W(CO)_5O_2CCH_3]$ with $P(OCH_3)_3$. The value at 30.0 °C is the average of three measurements.

Me₂THF as the solvent necessitated a change in counterion from PPN^+ to Et_4N^+ as the PPN^+ salt of the metal complex is insoluble in this solvent. $[Et_4N][W(CO)_5O_2CCH_3]$ is only moderately soluble in 2,5-Me₂THF.

Also measured were the kinetics of carbonyl substitution of $[PPN][W(CO)_5O_2CCH_3]$ by PPh_3 to yield $[PPN][W(CO)_4(PPh_3)O_2CCH_3]$. Pseudo-first-order conditions were employed with the phosphine concentration in large excess (>40-fold) over the metal complex. In a typical run, THF solutions of $[PPN][W(CO)_5O_2CCH_3]$ (0.080 g, 9.0×10^{-5} mol in 2.0 mL) and PPh_3 (0.90 g, 3.0×10^{-3} mol in 4.0 mL) were allowed to equilibrate to the desired temperature before the transfer of the phosphine solution into the $[PPN][W(CO)_5O_2CCH_3]$ solution via a cannula. The formation of $[PPN][W(CO)_4(PPh_3)O_2CCH_3]$ was fol-

(9) Darensbourg, D. J.; Rokicki, A.; Darensbourg, M. Y. *J. Am. Chem. Soc.* **1981**, *103*, 3223.

(10) Wiegreffe, P. W. Ph.D. Dissertation, Texas A&M University, College Station, TX, 1988.

(11) Darensbourg, D. J.; Morse, S.; Ovalles, C.; Pickner, H. C. *Inorg. Synth.*, in press.

(12) The value of k_{obs} was difficult to measure at 35.0 °C due to the fast reaction rate. At this temperature, k_{obs} was measured three times, and the average of the values was used as a single point in the Arrhenius plot.

(13) Before the kinetic determination was begun, the $[Et_4N][W(CO)_5O_2CCH_3]$ solution was cannulated away from undissolved $[Et_4N][W(CO)_5O_2CCH_3]$. The kinetics of these saturated solutions with $P(OCH_3)_3$ were monitored by following the disappearance of the 1910- cm^{-1} band instead of the appearance of the 2066- cm^{-1} peak, because solubility properties prevented the formation of more concentrated solutions. Concentrated solutions are necessary when following the 2066- cm^{-1} peak, because the intensity of this band is small. The rate constants were determined by plotting $\ln(A_i - A_t)$ vs time, where A_t is the absorbance at time t and A_i is the absorbance at infinite time.

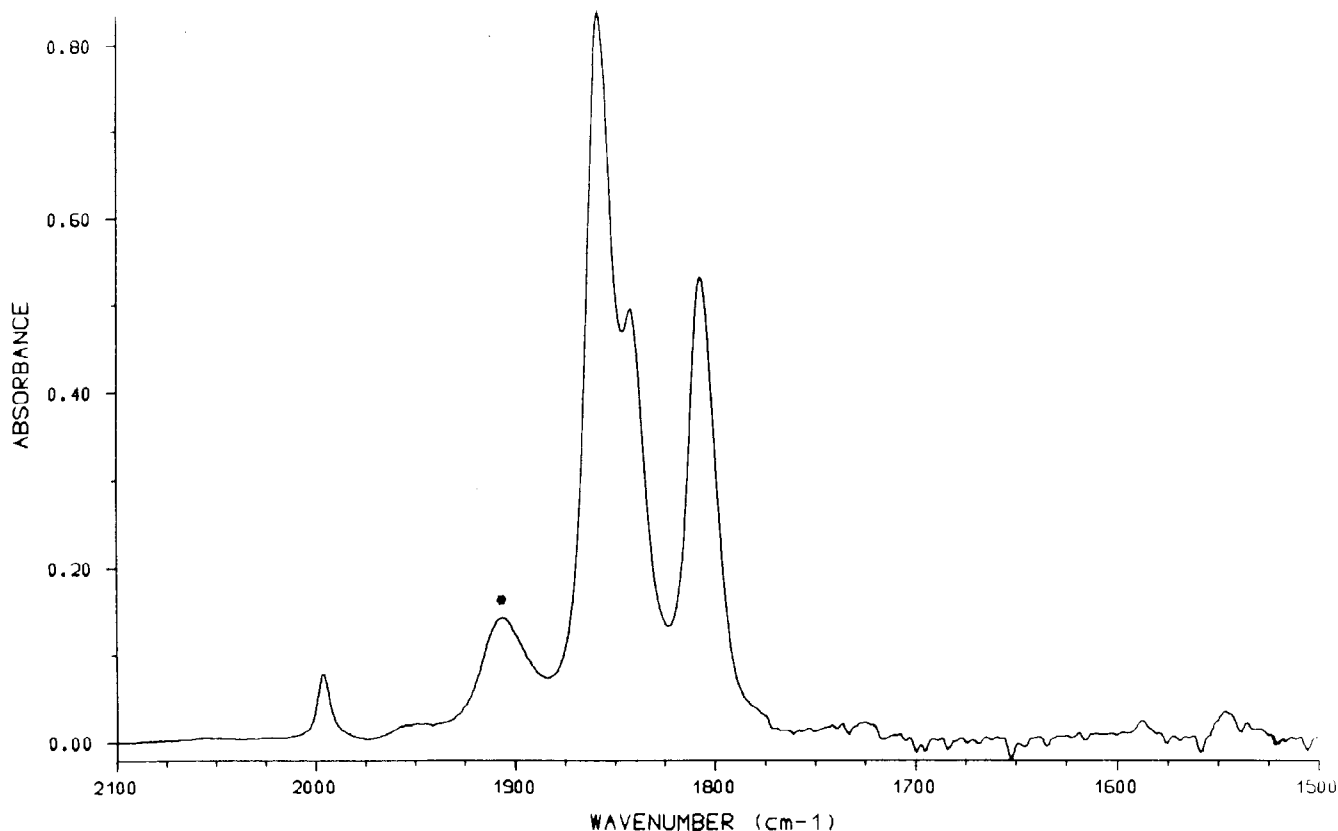


Figure 3. IR spectrum of $[\text{PPN}][\text{W}(\text{CO})_4(\eta^2\text{-O}_2\text{CCH}_3)]$. Note: the asterisk marks the $[\text{PPN}][\text{W}(\text{CO})_5\text{Cl}]$ impurity.

lowed by the appearance of the 1997-cm^{-1} band with a base-line correction made at 2030-cm^{-1} . Pseudo-first-order rate constants were calculated in the same fashion as those for the phosphite substitution reaction described above.

Equilibrium Constant Measurements. The equilibrium constant of the reaction between $[\text{PPN}][\text{W}(\text{CO})_5\text{O}_2\text{CCH}_3]$ and PPh_3 was measured by IR spectroscopy. A small quantity of $[\text{PPN}][\text{W}(\text{CO})_5\text{O}_2\text{CCH}_3]$ (0.080 g , $9.0 \times 10^{-5}\text{ mol}$) was dissolved in THF (6.0 mL). The absorbance of the E band (1906 cm^{-1}) was measured. To the solution, a known quantity of phosphine was added. After the nitrogen was evacuated, an atmosphere of CO was added and the solution was protected from light by covering the reaction vessel with foil. The solution was allowed to equilibrate with stirring for several hours. The decrease in absorbance of the $\nu(\text{CO})$ E band was measured. From a Beer's law plot of $[\text{PPN}][\text{W}(\text{CO})_5\text{O}_2\text{CCH}_3]$, its initial and equilibrium concentrations were determined. K_{eq} at room temperature was calculated from

$$K_{\text{eq}} = \frac{[\text{W}(\text{CO})_4(\text{PPh}_3)\text{O}_2\text{CCH}_3][\text{CO}]}{[\text{W}(\text{CO})_5\text{O}_2\text{CCH}_3][\text{PPh}_3]}$$

where the concentration of the phosphine-substituted product was assumed to be equal to $[\text{W}(\text{CO})_5\text{O}_2\text{CCH}_3]_{\text{initial}} - [\text{W}(\text{CO})_5\text{O}_2\text{CCH}_3]_{\text{final}}$. The concentration of CO dissolved in THF at room temperature was taken to be 0.0084 mol/L at 1 atm .¹⁴ The phosphine concentration at equilibrium was assumed to be equal to its original concentration, since a large excess (47-, 63-, and 81-fold) was used in each of the determinations.

By the same procedure, K_{eq} was determined for the reaction of $[\text{PPN}][\text{W}(\text{CO})_5\text{O}_2\text{CCH}_3]$ with $\text{P}(\text{OCH}_3)_3$.

Synthesis of $[\text{PPN}][\text{W}(\text{CO})_4(\eta^2\text{-O}_2\text{CCH}_3)]$. A THF solution of $[\text{PPN}][\text{W}(\text{CO})_5\text{O}_2\text{CCH}_3]$ (0.10 g , $1.0 \times 10^{-4}\text{ mol}$ in 50 mL) was placed in a water-jacketed photolysis vessel, and a vigorous stream of nitrogen was bubbled through the yellow solution. After 45–60 min of photolysis, an orange solution formed. The IR spectrum of this solution, shown in Figure 3, indicates the major component to be of C_{2v} symmetry, with an impurity, namely $[\text{PPN}][\text{W}(\text{CO})_5\text{Cl}]$, absorbance marked by an asterisk. Attempts to isolate the compound as a solid or to obtain X-ray quality crystals have thus far been unsuccessful. The complex decomposes in solution to form the starting material at room temperature in approximately 6 h and reacts rapidly with ligands (PPh_3 and CO) to form the substituted products $[\text{W}(\text{CO})_4(\text{L})\text{O}_2\text{CCH}_3]^-$.

Table I. Equilibrium Constants Determined for Various Concentrations of Phosphine for the Ligand Substitution Reaction of $[\text{PPN}][\text{W}(\text{CO})_5\text{O}_2\text{CCH}_3]$ with PPh_3 ^a

$10^3 K_{\text{eq}}$	$[\text{PPh}_3]$, M	molar excess of PPh_3
5.3	0.90	63
5.9	0.69	47
5.5	1.2	81

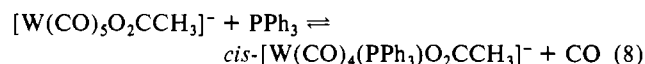
^a K_{eq} was measured under an atmosphere of CO at $25.0\text{ }^\circ\text{C}$.

Synthesis of $[\text{PPN}][\text{Cr}(\text{CO})_4(\eta^2\text{-O}_2\text{CH})]$. A THF solution of $[\text{PPN}][\text{Cr}(\text{CO})_5\text{O}_2\text{CH}]$ (0.070 g , $9.0 \times 10^{-5}\text{ mol}$ in 50 mL) was placed in a water-cooled photolysis vessel, and a vigorous stream of nitrogen was bubbled through the yellow solution. After the solution was cooled to $5\text{ }^\circ\text{C}$, it was photolyzed for 15 min. The $\nu(\text{CO})$ IR absorbances showed the solution to contain a mixture of $[\text{Cr}(\text{CO})_4(\eta^2\text{-O}_2\text{CH})]^-$ ($\nu(\text{CO})$ absorbances at 2002 (m) , 1871 (s) , 1852 (s) , and $1813\text{ (m)}\text{ cm}^{-1}$) and $[\text{Cr}(\text{CO})_5\text{O}_2\text{CH}]^-$. In solution, the chelated complex decomposed quickly to yield a solution that contained $[\text{Cr}(\text{CO})_5\text{O}_2\text{CH}]^-$ and a small quantity of $[\text{Cr}(\text{CO})_5\text{H}]^-$.

Synthesis of $\text{AgO}_2^{13}\text{CCH}_3$. To an aqueous solution of $\text{NaO}_2^{13}\text{CCH}_3$ (0.23 g , 0.0032 mol in 2.0 mL) was added dropwise an aqueous solution of AgNO_3 (0.53 g , 0.0032 mol in 2.0 mL). After being stirred for 10 minutes, the mixture was filtered and washed with copious amounts of distilled water, followed by washings with acetone. The solid was dried under vacuum overnight.

Results

Kinetic Experiments. For the reaction of $[\text{PPN}][\text{W}(\text{CO})_5\text{O}_2\text{CCH}_3]$ with PPh_3 (eq 8), K_{eq} was determined at a variety of phosphine concentrations (Table I). At $25.0\text{ }^\circ\text{C}$, K_{eq} was calculated to be $(5.54 \pm 0.30) \times 10^{-3}$.

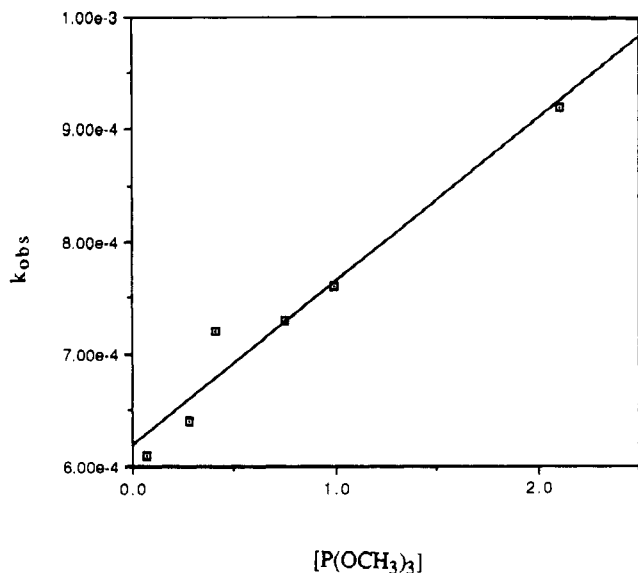


Under pseudo-first-order conditions, k_{obs} was found to be independent of triphenylphosphine concentration. As the small equilibrium constant for the reaction of $[\text{PPN}][\text{W}(\text{CO})_5\text{O}_2\text{CCH}_3]$ with PPh_3 prevented us from obtaining very reliable activation parameters for the forward reaction, we sought to change ligands from PPh_3 to an electronically and sterically more favorable ligand,

Table II. k_{obs} Determined in THF at a Variety of Phosphite Concentrations for the Ligand Substitution Reaction of $[\text{PPN}][\text{W}(\text{CO})_5\text{O}_2\text{CCH}_3]$ with $\text{P}(\text{OCH}_3)_3$

$10^4 k_{\text{obs}}, \text{s}^{-1}$	$[\text{P}(\text{OCH}_3)_3], \text{M}$	molar excess of $\text{P}(\text{OCH}_3)_3$
6.13 ± 0.24	0.071	5
6.40 ± 0.05	0.28	20
7.19 ± 0.12	0.41	40
7.27 ± 0.13	0.75	60
7.62 ± 0.12	0.99	80
9.24 ± 0.75	2.1	150

^aTemperature = 25.0 °C.

**Figure 4.** Plot of k_{obs} as a function of $\text{P}(\text{OCH}_3)_3$ concentration for the ligand substitution reaction of $[\text{PPN}][\text{W}(\text{CO})_5\text{O}_2\text{CCH}_3]$ with $\text{P}(\text{OCH}_3)_3$.

$\text{P}(\text{OCH}_3)_3$. Although the reaction of $\text{P}(\text{OCH}_3)_3$ with $[\text{PPN}][\text{W}(\text{CO})_5\text{O}_2\text{CCH}_3]$ was found to be an equilibrium process also, K_{eq} favored a greater amount of product formation. Indeed, K_{eq} was found to be approximately 170 times larger than the equilibrium constant with PPh_3 .

For the reaction of $[\text{PPN}][\text{W}(\text{CO})_5\text{O}_2\text{CCH}_3]$ and $\text{P}(\text{OCH}_3)_3$, the pseudo-first-order rate constant, k_{obs} , was measured as a function of phosphite concentration (Table II). From a range of phosphite concentrations of 0.07–2.1 M (5–150-fold excess of $\text{P}(\text{OCH}_3)_3$ over the metal complex concentration), a small linear dependence of k_{obs} on $[\text{P}(\text{OCH}_3)_3]$ was detected (Figure 4). From the least-squares analysis, k_{obs} was calculated for zero $\text{P}(\text{OCH}_3)_3$ concentration and found to be $6.2 \times 10^{-4} \text{ s}^{-1}$. Under pseudo-first-order conditions, with a $\text{P}(\text{OCH}_3)_3$ concentration approximately 20 times that of the metal complex, k_{obs} at room temperature was found to be $(6.4 \pm 0.06) \times 10^{-4} \text{ s}^{-1}$. Thus we conclude that under this condition the assumption that $k_{\text{obs}} \approx k_1$, the CO dissociation rate constant, is valid. In the absence of the small contribution from an I_d process, at $[\text{P}(\text{OCH}_3)_3] \gg [\text{CO}]$, k_{obs} reduces to k_1 (eq 9).

$$k_{\text{obs}} = \frac{k_1 k_2 [\text{PR}_3] + k_{-1} k_{-2} [\text{CO}]}{k_{-1} [\text{CO}] + k_2 [\text{PR}_3]} \quad (9)$$

An Arrhenius plot, Figure 2, was made by measuring k_{obs} at seven temperatures between 25.0 and 35.0 °C (Table III). From these data, ΔH^\ddagger and ΔS^\ddagger were calculated to be $23.3 \pm 0.8 \text{ kcal mol}^{-1}$ and $5.4 \pm 2.6 \text{ eu}$, respectively.

The rates of CO displacement in $[\text{PPN}][\text{W}(\text{CO})_5\text{O}_2\text{CCH}_3]$ and $[\text{Et}_4\text{N}][\text{W}(\text{CO})_5\text{O}_2\text{CCH}_3]$ by trimethyl phosphite were determined under pseudo-first-order conditions by IR spectroscopy. In THF at 32.0 °C, k_{obs} was found to be $(1.92 \pm 0.1) \times 10^{-3} \text{ s}^{-1}$, when PPN^+ is the counterion, and $(1.79 \pm 0.02) \times 10^{-3} \text{ s}^{-1}$, for the Et_4N^+ salt. As these rate constants do not differ greatly, the counterion has negligible effect on the value of k_{obs} .

To examine the rate dependence on solvent interactions, k_{obs} in THF was compared with k_{obs} in a more sterically hindered and

Table III. k_{obs} as a Function of Temperature for the Reaction of $[\text{PPN}][\text{W}(\text{CO})_5\text{O}_2\text{CCH}_3]$ with a 20-fold Excess of $\text{P}(\text{OCH}_3)_3$ ^a

$10^3 k_{\text{obs}}, \text{s}^{-1}$	temp, °C	$10^3 k_{\text{obs}}, \text{s}^{-1}$	temp, °C
0.640 ± 0.01	25.0	1.85 ± 0.06	31.9
1.10 ± 0.04	28.0	1.92 ± 0.10	32.0
1.50 ± 0.05	29.9	2.16 ± 0.10	33.5
1.73 ± 0.11	30.0	2.73 ± 0.65	35.0

^aThe value of k_{obs} at 35.0 °C is the average of three rates measured at this temperature.

less coordinating solvent: 2,5-Me₂THF. At 25.0 °C, k_{obs} was determined for the Et_4N^+ salt in both solvents and found to be $(5.92 \pm 0.29) \times 10^{-4} \text{ s}^{-1}$ in 2,5-Me₂THF and $(4.93 \pm 0.13) \times 10^{-4} \text{ s}^{-1}$ in THF. As the rate constants vary only slightly, it can be concluded that the solvent does not play a significant role in determining the value of k_{obs} .

For the carbonyl substitution reaction of $[\text{PPN}][\text{W}(\text{CO})_5\text{Cl}]$ with $\text{P}(\text{OCH}_3)_3$, k_{obs} was determined to be $(1.22 \pm 0.12) \times 10^{-3} \text{ s}^{-1}$ at 35.0 °C. This rate is less than half as fast as the reaction rate of $[\text{PPN}][\text{W}(\text{CO})_5\text{O}_2\text{CCH}_3]$ with $\text{P}(\text{OCH}_3)_3$.¹⁵

¹³C NMR Experiments. The ¹³C NMR spectrum of highly enriched $[\text{PPN}][\text{W}(\text{CO})_5\text{O}_2\text{CCH}_3]$ indicated the cis and trans carbonyls resonate at 202.1 and 206.3 ppm downfield from TMS, respectively.¹¹ As expected, the cis-carbonyl signal was split into a doublet and the trans signal into a quintet. Also observed in the spectrum were the appropriate tungsten satellites and resonances for $[\text{PPN}][\text{W}(\text{CO})_5\text{Cl}]$.^{11,16}

After photolysis of $[\text{PPN}][\text{W}(\text{CO})_5\text{O}_2\text{CCH}_3]$, the ¹³C NMR carbonyl region (Figure 5) showed two resonances of approximately equal intensity and split into triplets, at 206.4 and 217.8 ppm ($J_{\text{C-C}} = 3.1 \text{ Hz}$). The ¹³C resonances for $[\text{W}(\text{CO})_5\text{Cl}]^-$ were still observed as well as the tungsten satellites, but no $[\text{W}(\text{CO})_5\text{O}_2\text{CCH}_3]^-$ resonances were detected. The ¹³C NMR spectrum of $[\text{PPN}][\text{W}(\text{CO})_5\text{O}_2\text{CCH}_3]$ was examined under high-resolution conditions and no evidence of long-range coupling between the acetate carbon and the carbonyl carbon resonances was detected.

Infrared Experiments. The infrared spectrum of the product obtained upon photolysis of $[\text{PPN}][\text{W}(\text{CO})_5\text{O}_2\text{CCH}_3]$ in THF exhibited $\nu(\text{CO})$ stretching frequencies at 1998 (w), 1859 (s), 1843 (m), and 1808 (m) cm^{-1} , which are consistent with a $\text{W}(\text{CO})_4$ unit of C_{2v} symmetry. On the other hand, the nature of the bonding of the acetate ligand with the metal center (i.e., monodentate, chelating, or bridging) can be assessed from the different in the antisymmetric and symmetric stretching modes of the acetate ligand.¹⁷ In this regard, the IR spectrum of a concentrated solution of $[\text{PPN}][\text{W}(\text{CO})_5\text{O}_2\text{CCH}_3]$ in THF shows $\nu_a(\text{COO}^-)$ and $\nu_s(\text{COO}^-)$ absorptions at 1615 and 1368 cm^{-1} , respectively. While the value of $[\nu_a(\text{COO}^-) - \nu_s(\text{COO}^-)]$ in this instance is 247 cm^{-1} , consistent with a monodentate acetate ligand, the analogous spectrum of the photolysis product was inconclusive. The $\nu_a(\text{COO}^-)$ absorption was found to be 1546 cm^{-1} , but the $\nu_s(\text{COO}^-)$ band was difficult to assign, due to a poor solvent subtraction, in the region of interest.¹⁸ In order to shift the absorbances of the photolysis product into a region of the spectrum that is more amenable to this study, an investigation of $[\text{PPN}][\text{W}(\text{CO})_5\text{O}_2\text{CCH}_3]$ was undertaken.

The IR spectrum of the acetate region of $[\text{PPN}][\text{W}(\text{CO})_5\text{O}_2\text{CCH}_3]$ shows the $\nu_a(^{13}\text{COO}^-)$ and the $\nu_s(^{13}\text{COO}^-)$

- (15) (a) Allen, A. D.; Barrett, P. F. *Can. J. Chem.* **1968**, *46*, 1655. (b) Kudasroski-Hanckel, R. Ph.D. Dissertation 1985, Tulane University, New Orleans, LA, 1985; p 121.
- (16) The $[\text{PPN}][\text{O}_2\text{CCH}_3]$ used in the preparation of $[\text{PPN}][\text{W}(\text{CO})_5\text{O}_2\text{CCH}_3]$, is usually contaminated with $[\text{PPN}]\text{Cl}$. Under the reaction conditions necessary to synthesize $[\text{PPN}][\text{W}(\text{CO})_5\text{O}_2\text{CCH}_3]$, $[\text{PPN}][\text{W}(\text{CO})_5\text{Cl}]$ is produced.
- (17) Nakamoto, K. *Infrared and Raman Spectra of Inorganic and Coordination Compounds*, 4th ed.; John Wiley & Sons: New York, 1986; p 231.
- (18) The IR region from 1435 to 1465 cm^{-1} presents difficulties for this measurement, because the solvent (THF) absorbs strongly in this region. Attempts to change solvents failed because of similar absorptions or an inability to dissolve the metal complex.

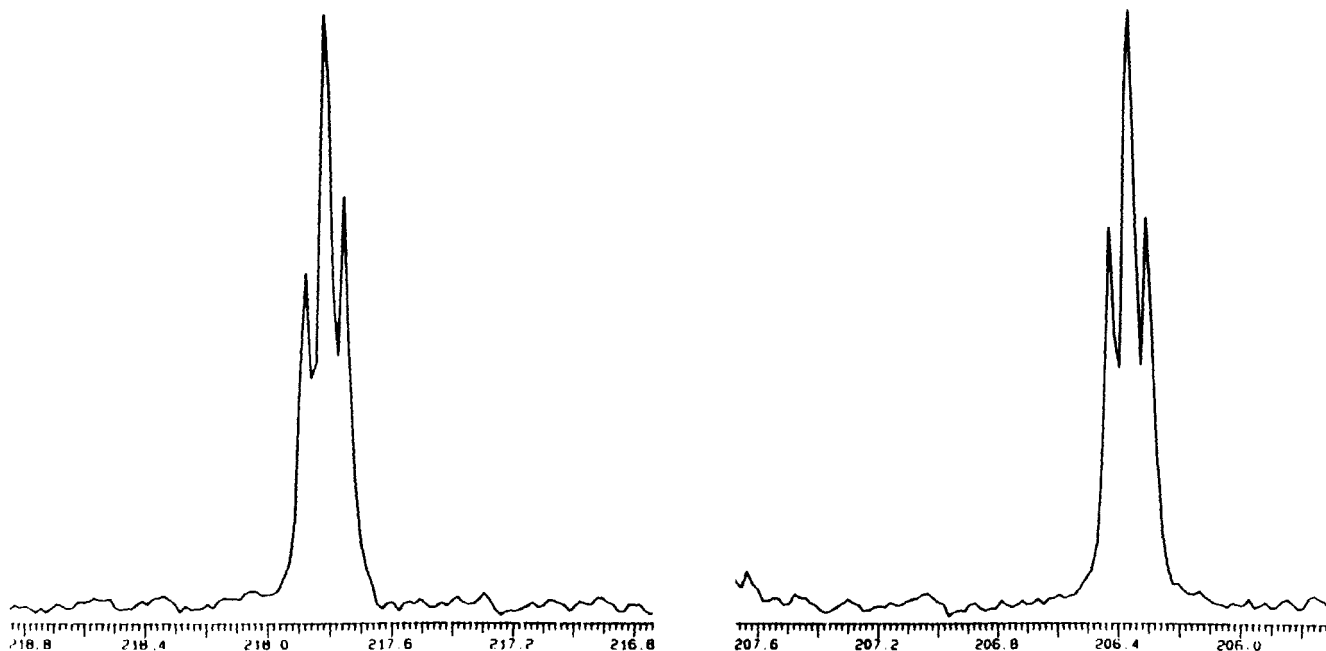


Figure 5. Carbonyl region of the ^{13}C NMR spectrum of $[\text{PPN}][\text{W}(^{13}\text{CO})_4(\eta^2\text{-O}_2\text{CCH}_3)]$.

absorbances at 1576 and 1354 cm^{-1} . The spectrum of the product resulting from photolysis of $[\text{PPN}][\text{W}(\text{CO})_5\text{O}_2\text{CCH}_3]$ shows the $\nu_a(^{13}\text{COO}^-)$ and the $\nu_s(^{13}\text{COO}^-)$ frequencies to be 1502 and 1426 cm^{-1} . Therefore, the difference between the two bands is 76 cm^{-1} , compatible with a chelating acetate ligand.¹⁷

Discussion

The substitution of a carbon monoxide ligand in the $[\text{W}(\text{CO})_5\text{O}_2\text{CCH}_3]^-$ anion by PPh_3 in tetrahydrofuran to afford *cis*- $[\text{W}(\text{CO})_4(\text{PPh}_3)\text{O}_2\text{CCH}_3]^-$ was shown to be a very facile process, obeying a rate law that is zero order in PPh_3 and first order in metal substrate. As anticipated for a dissociative pathway, the reaction was retarded by carbon monoxide. Indeed, in the presence of CO, the reverse reaction, dissociation of PPh_3 , occurs with equal facility, resulting in the establishing of an equilibrium (eq 8) with a K_{eq} value of $(5.54 \pm 0.30) \times 10^{-3}$ (or $\Delta G^\circ = +3 \text{ kcal mol}^{-1}$) at ambient temperature.

In order to accurately define the activation parameters for CO dissociation in $[\text{W}(\text{CO})_5\text{O}_2\text{CCH}_3]^-$, it was desirable to study a substitution reaction with a more favorable equilibrium position, i.e., a reaction that proceeded further to the right. This was achieved by employing the better π -acceptor and less sterically hindered trimethyl phosphite ligand as the incoming group. In this instance, the reaction was first order in metal substrate and exhibited a small dependence on $[\text{P}(\text{OCH}_3)_3]$ at high concentrations. This latter phenomenon is ascribed to a concurrent I_d process.¹⁹ Nevertheless, it was possible to determine the activation parameters for the phosphite-independent CO dissociation process, with $\Delta H^\ddagger = 23.3 \pm 0.8 \text{ kcal mol}^{-1}$ and $\Delta S^\ddagger = 5.4 \pm 2.6 \text{ eu}$.

The activation enthalpy for CO dissociation in $[\text{W}(\text{CO})_5\text{O}_2\text{CCH}_3]^-$ is significantly smaller than those reported for CO dissociation from $\text{W}(\text{CO})_6$ and $\text{W}(\text{CO})_5\text{PR}_3$ in hydrocarbon solvents,^{20,21} where $\Delta H^\ddagger = 39.9$ and 37.0 kcal mol^{-1} , respectively. One possible explanation would involve an I_d or I_a mechanism with the basic solvent THF to afford a solvated intermediate, *cis*- $[\text{W}(\text{CO})_4(\text{THF})\text{O}_2\text{CCH}_3]^-$, followed by rapid solvent replacement by the incoming phosphorus donor ligand. However, this is ruled out on the basis of the similarity in rate constants observed for CO substitution in $[\text{Et}_4\text{N}][\text{W}(\text{CO})_5\text{O}_2\text{CCH}_3]$ in THF and 2,5-dimethyltetrahydrofuran (2,5-Me₂THF) solvents. Molecular models clearly illustrate that it is not possible to form the cor-

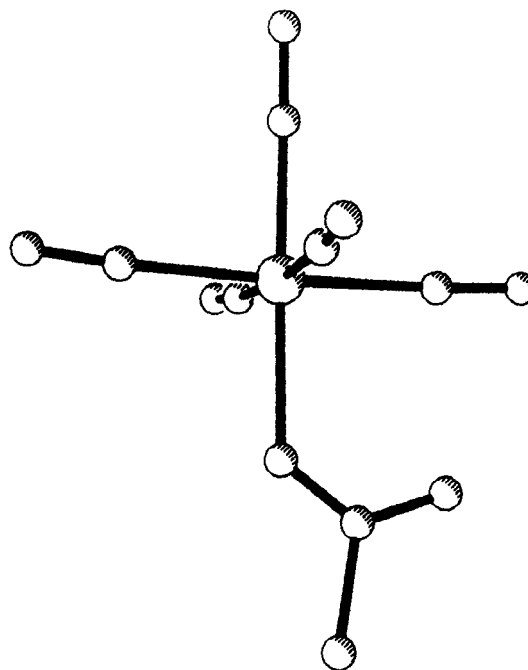


Figure 6. CHEM-X model of $[\text{W}(\text{CO})\text{O}_2\text{CCH}_3]^-$ with bond rotation through the tungsten-oxygen bond to minimize the C3 and O7 distance (2.56 Å).

responding solvent complex *cis*- $[\text{W}(\text{CO})_4(\text{S})\text{O}_2\text{CCH}_3]^-$ with the sterically hindered 2,5-Me₂THF solvent.

The use of the Et_4N^+ derivative in the above study was necessitated by the lack of solubility of the corresponding PPN^+ salt in 2,5-Me₂THF. Because strongly interacting counterions, e.g., Na^+ or Li^+ , are known to ion pair at the distal oxygen atom of the acetate moiety, leading to its displacement,^{22,23} it was important to ascertain whether interchanging PPN^+ with Et_4N^+ had an effect on the reactivity of the M-CO group. Indeed, this change in counterion had no significant effect on the rate of CO substitution as is evident by the similarity of the values of the rate constants for CO dissociation in the two salts in THF (vide supra).

An obvious alternative explanation, at least in part, for the enhanced CO lability in $[\text{W}(\text{CO})_5\text{O}_2\text{CCH}_3]^-$ is the involvement

(19) Darensbourg, D. J. *Adv. Organomet. Chem.* **1982**, *21*, 113.

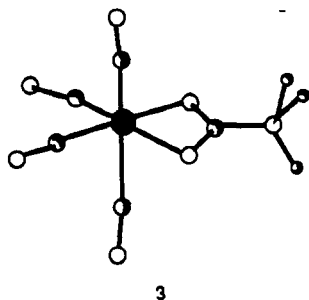
(20) Graham, J. R.; Angelici, R. J. *Inorg. Chem.* **1967**, *6*, 2082.

(21) Connor, J. A.; Day, E. M.; McEwen, G. K. *J. Chem. Soc., Dalton Trans.* **1973**, 347.

(22) Darensbourg, D. J.; Kudarowski, R. *J. Am. Chem. Soc.* **1984**, *106*, 3672.

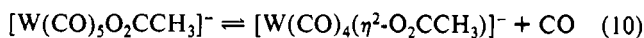
(23) Darensbourg, D. J.; Pala, M. *J. Am. Chem. Soc.* **1985**, *107*, 5687.

of an intramolecular acetate ligand-assisted CO displacement. Figure 6 depicts a view of the $[\text{W}(\text{CO})_5\text{O}_2\text{CCH}_3]^-$ anion with the acetate ligand rotated about its bond with tungsten with the CHEMX²⁴ graphics program to yield the closest contact (2.56 Å) between the distal oxygen atom and a cis ligand.¹ This distance is considerably shorter than the sum of the van der Waals radii (3.15 Å) of carbon (1.65 Å)²⁵ and oxygen (1.50 Å).²⁶ In the solid-state structure, the plane of the acetate ligand approximately bisects the two carbonyl (C4 and C3) ligands,² with the shortest distal oxygen (O7) to cis carbonyl C atoms (C4 and C3) contacts being 3.11 and 3.09 Å, respectively. Displacement of a cis CO ligand could then lead to chelate formation (species 3) prior to a facile reaction with incoming ligands (L) to afford the product $\text{cis-}[\text{W}(\text{CO})_4(\text{L})\text{O}_2\text{CCH}_3]^-$.

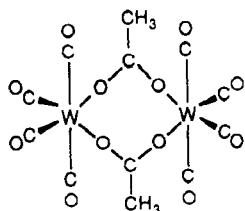


3

Infrared and ¹³C NMR spectroscopic evidence for the existence of species 3 has been obtained. Upon irradiation of a THF solution of $[\text{PPN}][\text{W}(\text{CO})_5\text{O}_2\text{CCH}_3]^-$ under a continuous sweep of nitrogen, formation of the $[\text{W}(\text{CO})_4(\eta^2\text{-O}_2\text{CCH}_3)]^-$ anion results by way of reaction 10. The infrared spectrum in the $\nu(\text{CO})$ region



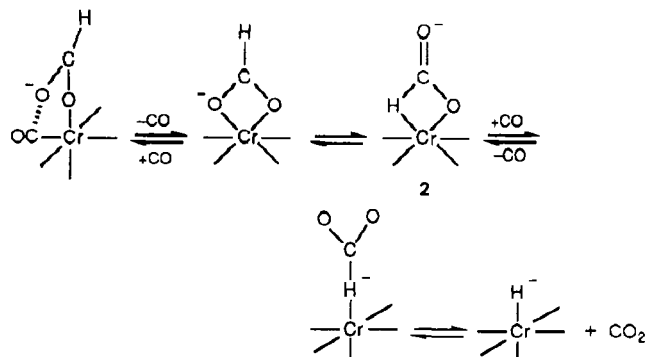
of the THF solution exhibited a four-band pattern indicative of a C_{2v} $[\text{W}(\text{CO})_4]$ moiety. Similarly, the ¹³C NMR spectrum of the solution emanating from reaction 10 using $[\text{W}^{13}\text{CO}]_5\text{O}_2\text{CCH}_3^-$ revealed that there were only two types of carbonyl ligands; i.e., two carbon resonances were observed of equal intensity, each being split into triplets as a consequence of coupling to two equivalent carbon atoms (Figure 5). This latter observations would rule out solvated species such as $\text{cis-}[\text{W}(\text{CO})_4(\text{THF})\text{O}_2\text{CCH}_3]^-$.^{27,28} Furthermore, the infrared spectrum in the carboxylate region, substantiated by ¹³C-substitution data, indicated the difference between $\nu_a(\text{COO}^-)$ and $\nu_s(\text{COO}^-)$ to be only 76 cm^{-1} , that expected for a *chelating* acetate ligand.¹⁷ This infrared probe eliminates the alternative structure assignment for species 3, that of a dimeric species, 4, containing bridging acetate ligands, where the $\nu_a(\text{COO}^-)$ and $\nu_s(\text{COO}^-)$ difference is anticipated to be much greater than 76 cm^{-1} .



4

- (24) CHEMX, developed and distributed by Chemical Design Ltd., Oxford, England.
 (25) Allinger, N. L.; Hirsch, J. A.; Miller, M. A.; Tyminski, I. J.; Van-Catledge, F. A. *J. Am. Chem. Soc.* **1968**, *90*, 1199.
 (26) Bondi, A. *J. Phys. Chem.* **1964**, *68*, 441.
 (27) In a previous study, we have indeed mistakenly assigned species 3 to the solvated intermediate, $\text{cis-}[\text{W}(\text{CO})_4(\text{THF})\text{O}_2\text{CCH}_3]^-$, on the basis of infrared spectral evidence in the $\nu(\text{CO})$ region only.²⁸
 (28) Tooley, P. A.; Ovalles, C.; Kao, S. C.; Darenbourg, D. J.; Darenbourg, M. Y. *J. Am. Chem. Soc.* **1986**, *108*, 5465.

Scheme I



The reaction of $[\text{W}(\text{CO})_4(\eta^2\text{-O}_2\text{CCH}_3)]^-$ with CO or phosphorus donor ligands occurs within time of mixing to yield the corresponding $\text{cis-}[\text{W}(\text{CO})_4(\text{L})\text{O}_2\text{CCH}_3]^-$ (L = CO or PR_3) products. Hence, it is highly likely that $[\text{W}(\text{CO})_4(\eta^2\text{-O}_2\text{CCH}_3)]^-$ is an intermediate in the ligand substitution reactions. That is, the process leading to formation of $[\text{W}(\text{CO})_4(\eta^2\text{-O}_2\text{CCH}_3)]^-$ might be a concerted one in which an unsaturated species such as $[\text{W}(\text{CO})_4(\eta^1\text{-O}_2\text{CCH}_3)]^-$ has no real lifetime.

It is worth noting at this point that the infrared spectra in the $\nu(\text{CO})$ region of THF solutions of $[\text{Cr}(\text{CO})_5\text{O}_2\text{CCH}_3]^-$ and $[\text{Mo}(\text{CO})_5\text{O}_2\text{CCH}_3]^-$ at ambient temperature, where CO dissociation requires less energy than for the tungsten derivative, display in addition to the major peaks of the parent complexes $\nu(\text{CO})$ bands corresponding to the $[\text{M}(\text{CO})_4(\eta^2\text{-O}_2\text{CCH}_3)]^-$ (M = Cr, Mo) derivatives. Formation of these chelated complexes became more evident upon heating each solution. The tungsten analogue does not form detectable quantities of the chelated species at ambient temperature; however, when it is refluxed in dimethoxyethane, a small quantity of the chelated complex can be identified by its $\nu(\text{CO})$ bands in the IR spectrum.

The identification of these $[\text{M}(\text{CO})_4(\eta^2\text{-O}_2\text{CCH}_3)]^-$ species raises an interesting question in the decarboxylation mechanism of the $[\text{M}(\text{CO})_5\text{O}_2\text{CH}]^-$ analogues, where the intermediacy of $[\text{M}(\text{CO})_4\text{O}_2\text{CH}]^-$ is conceivable.²⁹ That is, reaction 7 could contain the added step of formate chelate formation on route to the rate-determining step, which involves formation of species 2 (Scheme I). This in turn would suggest that O,O-chelate formation is a less energetic process than formation of species 2, which leads to decarboxylation. In fact, $[\text{Cr}(\text{CO})_4(\eta^2\text{-O}_2\text{CH})]^-$ has been identified by its $\nu(\text{CO})$ stretches in the IR spectrum after the photolysis of $[\text{Cr}(\text{CO})_5\text{O}_2\text{CH}]^-$ in THF at 5 °C. Furthermore, decarboxylation should be retarded by added carbon monoxide. This suggestion is evident from detailed investigations of the decarboxylation reaction, which will be the subject of an upcoming publication.^{10,30} For example, the free energy of activation (ΔG^\ddagger) for the decarboxylation of $[\text{Cr}(\text{CO})_5\text{O}_2\text{CH}]^-$ has been determined to be 23.1 kcal mol^{-1} , with the corresponding value for the tungsten analogue being qualitatively observed to be much higher.³⁰ Simultaneously, the ΔG^\ddagger determined herein for $[\text{W}(\text{CO})_4(\eta^2\text{-O}_2\text{CCH}_3)]^-$ formation from $[\text{W}(\text{CO})_5\text{O}_2\text{CCH}_3]^-$ is 21.7 kcal mol^{-1} , with the analogous free energy of activation for $[\text{Cr}(\text{CO})_5\text{O}_2\text{CCH}_3]^-$ expected to be smaller.

Acknowledgment. The financial support of this research by the National Science Foundation (Grants CHE 86-03681 and CHE 88-17873) and the Robert A. Welch Foundation is greatly appreciated.

Registry No. $[\text{W}(\text{CO})_5\text{O}_2\text{CCH}_3]^-$, 45146-15-4; $[\text{W}(\text{CO})_4(\eta^2\text{-O}_2\text{CCH}_3)]^-$, 124687-16-7; $[\text{PPN}][\text{W}(\text{CO})_4(\eta^2\text{-O}_2\text{CCH}_3)]^-$, 124687-17-8; $[\text{PPN}][\text{Cr}(\text{CO})_4(\eta^2\text{-O}_2\text{CH})]^-$, 124687-19-0; $\text{Ag}_2^{13}\text{CCH}_3$, 84174-88-9; $\text{P}(\text{OCH}_2\text{CH}_3)_3$, 121-45-9; PPh_3 , 603-35-0; CO, 630-08-0.

- (29) Darenbourg, D. J.; Wiegrefe, P. W. To be submitted for publication.
 (30) For a theoretical treatment of this CO_2 insertion reaction, see: Bo, C.; Dedieu, A. *Inorg. Chem.* **1989**, *28*, 304.